33RD INTERNATIONAL COSMIC RAY CONFERENCE, RIO DE JANEIRO 2013
THE ASTROPARTICLE PHYSICS CONFERENCE

ICRC 2013

Angular distribution of Cherenkov photons from air showers initiated by protons, iron nuclei or photons of energies from 10 TeV to 10 EeV in the presence of the geomagnetic field

P. HOMOLA[1,2], R. ENGEL[3], H. WILCZYŃSKI[2]

[1] *University of Siegen, Germany*
[2] *H. Niewodniczański Institute of Nuclear Physics PAN, Kraków, Poland*
[3] *Karlsruhe Institute of Technology, Germany*

homola@hep.physik.uni-siegen.de

Abstract: The angular distribution of Cherenkov light in an air shower is closely linked to that of the shower electrons and positrons. As charged particles in extensive air showers are deflected by the magnetic field of the Earth a deformation of the Cherenkov light distribution, that would be approximately symmetric about the shower axis if no magnetic field were present, is expected. In this work we study the variation of the Cherenkov light distribution as a function of the azimuth angle in the plane perpendicular to shower axis. It is found that the asymmetry induced by the geomagnetic field is most significant for early stages of showers arriving almost perpendicularly to the vector of the local geomagnetic field. It is shown that ignoring the azimuthal asymmetry of Cherenkov light might lead to a significant under- or overestimation of the Cherenkov light signal especially at sites where the local geomagnetic field is strong. Based on CORSIKA simulations, the azimuthal distribution of Cherenkov light is parametrized in dependence on the magnetic field component perpendicular to the shower axis and air density. This parametrization provides an efficient approximation for estimating the asymmetry of the Cherenkov light distribution for shower simulation and reconstruction in cosmic ray and gamma-ray experiments in which the Cherenkov signal of showers is observed.

Keywords: Extensive air showers, Cherenkov light, azimuthal asymmetry, geomagnetic field.

1 Introduction

Many imaging and non-imaging techniques of observing high-energy air showers are based on the detection of the abundant number of photons produced by Cherenkov radiation of the secondary electrons and positrons in these showers (see, for example, [1, 2, 3, 4, 5]). Cherenkov light also constitutes an important contribution [6] to the optical signal recorded by fluorescence telescopes built for the observation of very high energy showers [7, 8, 9, 10].

With a typical Cherenkov angle of the order of 1° in air, the angular distribution of Cherenkov light around the shower axis reflects the angular distribution of the charged particles, mainly electrons and positrons. A proper estimation of angular distribution of the Cherenkov light produced at various stages of the shower evolution is important for the reconstruction of the shower observables and, hence, the parameters of the primary particle.

At high shower energies, the energy, angular, and lateral distributions of $e^{\pm}$ exhibit universality features and can be expressed as function of the shower age and lateral distance in Moliere units, e.g. [11, 12, 13, 14, 15, 16, 17, 18]. Based on universality considerations several parametrizations of the angular distribution of Cherenkov light have been derived, see [11, 7, 15, 19]. In these studies, the angular distribution of Cherenkov photons is considered as approximately symmetric about the shower axis and the influence of the local magnetic field has been neglected. The effects of the geomagnetic field have been studied so far only for primary photons with energies of about 10^{12} eV [20].

The purpose of this work is the quantification of the expected asymmetry of the Cherenkov light distribution of air showers of very high energy. Using CORSIKA simulations a parametrization of the angular asymmetry induced by the geomagnetic field is derived for air showers from TeV energies up to the highest energies. Considering different local magnetic field strengths and shower geometries it is discussed under what conditions this asymmetry needs to be taken into account.

In this paper we show how the asymmetry of the azimuthal distribution of Cherenkov photons varies for different shower parameters and geomagnetic conditions. We replace the commonly used angular distribution of Cherenkov photons dependent only on the viewing angle to the shower axis, $F(\theta)$, with a more accurate function dependent also on the azimuthal angle in the plane perpendicular to the shower axis, $F(\theta,\phi)$. We develop an efficient parametrization that can be used at an arbitrarily selected experimental site with a given local geomagnetic field vector. As an example, the location of the Tunka experiment [3] (51° 48' N, 103° 04' E) is considered. In this experiment a surface array of non-imaging photon detectors is used to record the Cherenkov light emitted by extensive air showers of energies between 10^{14} eV and 10^{17} eV. The geomagnetic field at the site is exceptionally strong ($B = 0.6$ G), which should allow experimental verification of the results of this study.

2 Universality of electron and Cherenkov photon distributions

For showers of very high energies, the lateral distribution of charged particles can be well described as a universal function of the primary energy E_0, the lateral distance in

Moliere units, and the approximate shower age $s = 3/(1 + 2X_{\max}/X)$, where X is the atmospheric slant depth in g/cm^2 and $X_{\max}$ is the slant depth of shower maximum. There are some differences for different primary particles that are related to hadronic interactions at low energy, see [17, 18]. And, through the altitude dependence of the Moliere unit, there is also a dependence on the atmospheric density profile.

This universality is violated to some extent by the asymmetry implied by the local geomagnetic field. Averaged over local azimuth angle, the electron lateral distributions of high-energy showers are known not to depend significantly on s (in the range of $0.7 < s < 1.2$), E_0 nor on the primary type – if the primary is a nucleus (see e.g. [14, 15, 17]). For non-hadronic primaries, some differences in the shapes of these distributions are expected [17]. The universality of the relevant distributions were checked with CORSIKA [21] for different energy intervals and different primary particles, including photons. The comparison shows no significant differences of the angular distributions of electrons of energies of relevance to Cherenkov light production. Differences found for the higher energy ranges are related to shower-to-shower fluctuations and statistical fluctuations due to the limited number of particles in these histograms. The universality of the electron distributions leads to a similar universality of the angular distribution of Cherenkov photons. Parametrizations of this distribution as a function of shower age and height can be found e.g. in [15] and [22]. These parametrizations are very good approximations of the true angular distribution if the local geomagnetic field component perpendicular to the shower axis is small or if one considers distributions averaged over the azimuthal angle relative to the shower axis.

3 Parametrization of azimuthal Cherenkov light distribution

The universality of the underlying electron and positron distributions implies that the azimuthal profiles of Cherenkov photons can also be described by a universal function if expressed in suitable variables. Following Elbert *et al.* [20], we make the ansatz that the asymmetry of the azimuthal profile of Cherenkov photons can be described by a function of the local azimuth angle (ϕ), the angle to shower axis (θ) and the parameter a defined as

$$a = B_{\perp}/\rho, \tag{1}$$

where ρ is the local air density. A dependence on the air density is expected due to multiple Coulomb scattering. In addition the energy threshold for Cherenkov emission depends on the air density through the density dependence of the refractive index $n = n(\rho)$. We assume that the variation of n with wavelength λ is negligible for $300\,\text{nm} < \lambda < 400\,\text{nm}$.

In the following we consider proton, nuclei, and photon induced showers in the energy range $10^{15} < E_0/eV < 10^{17}$ eV and focus on the shower ages s that are of relevance to shower detection $0.7 < s < 1.2$. The Monte Carlo simulations were carried out with CORSIKA 6.970 [21] and COAST 3.01 with *root rack* option [24]. COAST (COrsika dAta accesS Tools) is a library of C++ routines providing simple and standardized access to CORSIKA data. Generally, COAST can be used to analyze every particle and interaction that occurs in an air shower generated with CORSIKA and is particularly well-suited to sample shower particles on arbitrary geometries[1]. The COAST option *root rack* enables histogramming shower particles within user-defined planes perpendicular to the shower axis. All the shower simulations used for deriving the parametrization were made with 40 observational levels spaced by a constant atmospheric depth interval ΔX.

The arrival directions of simulated showers are specified in the frame of reference used in CORSIKA. This means that the shower azimuth is counted counter-clockwise beginning from geomagnetic South, e.g. a shower coming from geomagnetic South has the azimuth $\phi_0 = 0^\circ$ and the one coming from geomagnetic East has the azimuth $\phi_0 = 90^\circ$. In addition, a local frame related to the shower axis is used. It is centered at the shower core at a given observation level (e.g. ground) and its z-axis points downwards along the shower axis while the x-axis is defined by the direction of the component of the local geomagnetic field vector transverse to the shower axis. The local azimuth is counted clockwise. All the simulations were performed using the US Standard Atmosphere density profile [25].

For the purpose of deriving a parametrization of the azimuthal distributions of Cherenkov photons, we simulated proton-induced showers with three primary energies (10^{15}, 10^{16} and 10^{17} eV) arriving at two different zenith angles (58° and 70°) for different values of $B_{\perp}$ (0.2, 0.3, 0.4, 0.5, and 0.6 G). These simulation parameters were selected to cover a reasonably wide range of the parameter a and to ensure acceptable computing time for producing the shower library. Of the 40 observation levels the first of them is always located at the top of the atmosphere which corresponds to a height of 100 km in CROSIKA. To obtain an azimuthal distribution of the emitted Cherenkov radiation for segments of the shower, we histogram photons emitted between the two adjacent observational planes at a given angle to shower axis (θ). The width of the binning in θ is 2°, while the bin width of the local azimuth ϕ is 10°. After a simulation run each histogram is normalized to 1. For each combination of primary energy, arrival direction and $B_{\perp}$, a simulation run was repeated 10 times with different random seed initialization. An example of a histogram of Cherenkov photons is shown in Fig. 1.

In the next step of the analysis we process each of the selected histograms to find the heights of the peaks related to positrons (B_{e^+}) and electrons (B_{e^-}) (see Fig. 1). The values of B_{e^+} and B_{e^-} depend on a and θ. An example of this dependence is shown in Fig. 2, where B_{e^+} is plotted as a function of a for 2 different viewing angles θ. For each histogram of Cherenkov photons an average value of a is calculated based on the atmospheric air density ρ at the two levels determining the histogram, with interpolation of ρ. The maximum uncertainty of this interpolation is reflected in the horizontal error bars. Fig. 2 indicates that the azimuthal asymmetry increases with a and θ.

The increase of B_{e^+} with a means that the asymmetry is larger for stronger $B_{\perp}$ or for smaller air density. A stronger $B_{\perp}$ leads to a stronger deflection of the trajectories of charged particles, hence the asymmetry of the az-

1. It has to be noted that Cherenkov photons cannot be analyzed directly with the original version of COAST. For the purpose of this study a few dedicated modifications were introduced into both the CORSIKA and COAST codes in order to enable histogramming of Cherenkov photons.

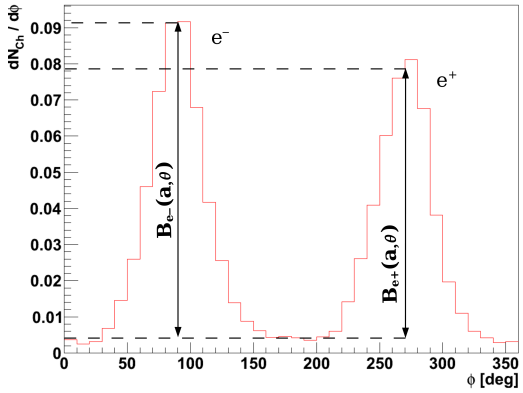

Fig. 1: Example histogram of Cherenkov photons from one of the simulations used for deriving the parametrization. The histogram was obtained for a proton primary of energy 10^{15} eV arriving at a zenith angle of 70°, with $B_\perp$=0.6 G. Only photons emitted at an average shower age $s = 0.8$ and viewing angle $14^\circ < \theta < 16^\circ$ are shown. In this case $a = 2.9\,\mathrm{Gm^3 kg^{-1}}$.

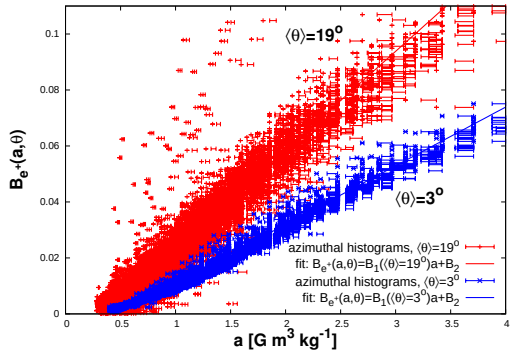

Fig. 2: Dependence of peak height $B_{e^+}(a,\theta)$ of normalized azimuthal Cherenkov profiles on asymmetry parameter a for different simulation parameters for two different angles θ. The symbols with error bars represent the simulation results used for the fit. For other details and parameters of the fitted functions see the text.

imuthal profile of Cherenkov photons is more pronounced than in case of weaker $B_\perp$. At the same time the mean free path of electrons over which they are being deflected increases with decreasing air density which also causes an increase of the azimuthal asymmetry of Cherenkov photons. Finally, the increase of this asymmetry with θ is related to the number of electrons of different energies varying with θ. At larger viewing angles one expects more low energy electrons than close to the axis. The low energy electrons are deflected by the geomagnetic field more efficiently than charged particles of higher energies.

However, for angles θ exceeding $\sim 30^\circ$, the energy of the electrons is often below the threshold for the Cherenkov emission, leading to a decrease of the Cherenkov photon asymmetry at larger angles. On the other hand, the intensity of the Cherenkov light emitted at large viewing angles is negligible in comparison to the Cherenkov light emitted at smaller angles but scattered to large viewing angles in the atmosphere. As will be discussed below, we do not consider viewing angles larger than 20° for deriving a parametrization of the asymmetry.

The numerically found values of B_{e^+} and B_{e^-} can be described by a linear function of the parameter a

$$B_{e^+/e^-}(a,\theta) = B_1(\theta)a + B_2$$
$$B_1(\theta) = B_{11}\theta^2 + B_{12}\theta + B_{13}, \quad (2)$$

where

$$B_2(e^+) = -0.0093 \pm 0.0004$$
$$B_{11}(e^+) = (-6.2 \pm 0.5)10^{-5}\mathrm{deg}^{-2}$$
$$B_{12}(e^+) = (0.0022 \pm 0.0001)\mathrm{deg}^{-1}$$
$$B_{13}(e^+) = 0.0136 \pm 0.0005, \quad (3)$$

and

$$B_2(e^-) = -0.0084 \pm 0.0005$$
$$B_{11}(e^-) = (-8.5 \pm 0.5)10^{-5}\mathrm{deg}^{-2}$$
$$B_{12}(e^-) = (0.0028 \pm 0.0001)\mathrm{deg}^{-1}$$
$$B_{13}(e^-) = 0.0124 \pm 0.0005. \quad (4)$$

The normalized distribution can be approximated by

$$F(a,\theta,\phi) = A + F_S(a,\theta)[1 + F_A(a,\theta)\sin\phi]\,\sin^4\phi, \quad (5)$$

where $A = 1/(2\pi) - 3F_S/8$ is the normalization constant and coefficients $F_S(a,\theta)$ and $F_A(a,\theta)$ are given by the heights of the distribution peaks B_{e^+} and B_{e^-}

$$F_S(a,\theta) = [B_{e^-}(a,\theta) + B_{e^+}(a,\theta)]/2,$$
$$F_A(a,\theta) =$$
$$[B_{e^-}(a,\theta) - B_{e^+}(a,\theta)]/[B_{e^-}(a,\theta) + B_{e^+}(a,\theta)]. \quad (6)$$

As mentioned earlier, the density of Cherenkov photons decreases rapidly with increasing θ. Therefore the quality of the azimuthal histograms at large viewing angles θ is limited by statistics. Also for small θ angles (near the shower axis) the densities of electrons (and hence of the Cherenkov photons) are low due to electromagnetic scattering. As a consequence, the histograms collected for this analysis allowed us to investigate only the limited range of the viewing angle of $2^\circ < \theta < 20^\circ$.

The parametrization was tested with a set of reference showers generated for the geomagnetic location of the Tunka Cherenkov array. Performing a χ^2 test it is found that about 90% of all simulated histograms deviate less than 30% from the predicted asymmetry for photon-induced showers of primary energies $E_0 \geq 10^{14}$ eV, for showers initiated by protons with $E_0 \geq 10^{15}$ eV, and for iron-initiated showers with $E_0 \geq 10^{16}$ eV. The deviation of a histogram is considered to be less than 30% if the χ^2, calculated by assuming a 30% uncertainty for each interval of the histogram, is less than unity per degree of freedom. For example, the comparison of 50 histograms of proton-induced showers of 10^{14} eV with the parametrization is shown in Fig. 3.

The shower-to-shower fluctuations are rapidly decreasing with increasing energy. This improves the overall description of the azimuthal Cherenkov asymmetry. Deviations between the simulation results and the parametrization are found for the minima of the distribution. One would have to introduce further degrees of freedom in the

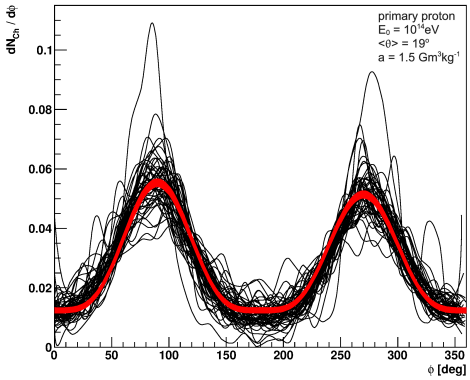

Fig. 3: Example of shower-to-shower fluctuations of azimuthal distributions of Cherenkov photons in air showers initiated by primary protons of energies $E_0 = 10^{14}$ eV. The thin black lines represent 50 simulated air showers and are compared to the parametrization (5) for $a = (1.5 \pm 3\%)$ Gm^{3}kg^{-1} and $< \theta >= 19^\circ$ (thick red lines).

parametrization (5) to obtain a better description of this part.

In this study, the statistics of histograms are sufficient to confirm the general applicability of the parametrization (5) in the range $0.3\,\mathrm{Gm^3kg^{-1}} < a < 2.5\,\mathrm{Gm^3kg^{-1}}$. Another study and more computing time are needed to determine the range of validity of parametrization (5) for larger a. Asymmetric profiles at small a are less interesting because they can hardly be distinguished from a flat distribution in azimuth.

It is important to note that the precision of the prediction (5), although satisfactory within the checked range of the parameter a, decreases with increasing a. This suggests that the application to the largest asymmetries of azimuthal Cherenkov distributions (expected for very large values of a) have to be considered with care. Further studies will be needed for showers of low energy, reaching their maxima at high altitudes (small ρ) and with large $B_\perp$. It is expected that, in such cases, the peaks in the azimuthal distributions will be narrower than the ones predicted by Eq. (5).

4 Summary and outlook

In this paper a detailed parametrization of the azimuthal asymmetry of the angular distribution of Cherenkov photons in high-energy showers was derived (Eq. 5). The parametrization can be applied to estimate the asymmetry for geomagnetic field strengths and air densities, expressed by the parameter a as $0.3\,\mathrm{Gm^3kg^{-1}} < a < 2.5\,\mathrm{Gm^3kg^{-1}}$. Such a wide range in a ensures that an azimuthal asymmetry of Cherenkov photons can be predicted well for the majority of showers in relevant experiments.

The result shows that the asymmetry of the azimuthal Cherenkov distribution caused by the geomagnetic field is expected to be significant when the air density is small and the local magnetic field component transverse to the shower axis is strong (large a). The asymmetry increases also with the angle between the viewing direction and the shower axis. Ignoring the asymmetry of azimuthal distributions of Cherenkov photons can lead to under- or overestimation of the Cherenkov component in the shower light profiles by up to one order of magnitude in the most extreme case.

One might consider an example simulation for a "worst case scenario" at a certain site. Let's define the maximum asymmetry of the azimuthal Cherenkov light distributions as $(dN_{ch}/d\phi)_{\phi=90^\circ}/(dN_{ch}/d\phi)_{\phi=180^\circ}$ and let's consider $10^{18.5}$eV proton showers arriving at the Auger site [9] from geographical South at zenith angles of 30° and 60°. If one looks at the maxima ($s = 1.0$) of these showers at a viewing angle of 15°, the expected asymmetries of the azimuthal Cherenkov light distributions are 1.04 and 1.15, respectively. For $s = 0.8$ the asymmetries are even larger: 1.20 and 1.39. For the TA site [10], where the local geomagnetic field is twice as strong as that at the Auger site, the expected asymmetries for showers seen at their maxima at a viewing angle of 15° and arriving at the same zenith angles and from geographical North are 1.45 for 30° and 2.45 for 60°. The respective asymmetries seen at $s = 0.8$ are 1.71 and 3.72.

The results of this work are important for high energy cosmic ray experiments in which the Cherenkov signal of showers is recorded and the local geomagnetic field is not very weak. As the parametrization formulas derived in this paper are applicable also for photon air showers of primary energies down to 10-100 TeV, they could also be used in the analysis of data from ground-based very high energy gamma-ray detectors.

Acknowledgments: This work was partially supported by the Polish Ministry of Science and Higher Education under grant No. NN 202 2072 38 and in Germany by the DAAD, project ID 50725595, by the Helmholtz Alliance for Astroparticle Physics and by the BMBF Verbundforschung Astroteilchenphysik.

References

[1] M. Cassidy *et al.*, arXiv:astro-ph/9707038 [astro-ph].
[2] B. Antokhonov *et al.* (TUNKA Collab.), Nucl. Instrum. Meth. A628 (2011) 124.
[3] S. Berezhnev *et al.* (Tunka Collab.), Nucl. Instrum. Meth. A692 (2012) 98.
[4] M. Tluczykont *et al.*, Adv. Space Res. 48 (2011) 1935.
[5] H. J. Völk and K. Bernlöhr, Exper. Astron. 25 (2009) 173.
[6] M. Unger *et al.*, Nucl. Instrum. Meth. A588 (2008) 433.
[7] R. M. Baltrusaitis *et al.* (Fly's Eye Collab.), Nucl. Instrum. Meth. A240 (1985) 410.
[8] J. Boyer *et al.*, Nucl. Instrum. Meth. A482 (2002) 457.
[9] J. A. Abraham *et al.* (Pierre Auger Collab.), Nucl. Instrum. Meth. A620 (2010) 227.
[10] H. Tokuno *et al.* (TA Collab.), Nucl. Instrum. Meth. A676 (2012) 54.
[11] A. M. Hillas, J. Phys. G8 (1982) 1461.
[12] A. M. Hillas, J. Phys. G8 (1982) 1475.
[13] M. Giller *et al.*, J. Phys. G30 (2004) 97.
[14] M. Giller *et al.* J. Phys. G31 (2005) 947.
[15] F. Nerling *et al.*, Astropart. Phys. 24 (2006) 421.
[16] P. Lipari, Phys. Rev. 79 (2008) 063001
[17] S. Lafebre *et al.*, Astropart. Phys. 31 (2009) 243.
[18] M. Ave *et al.*, Proc. of 31th Int. Cosmic Ray Conf., Beijing (2011) #1025.
[19] M. Giller and G. Wieczorek, Astropart. Phys. 31 (2009) 212.
[20] J. W. Elbert, T. Stanev, and S. Torii, Proc. of 18th Int. Cosmic Ray Conf., Bangalore 6 (1983) 227.
[21] D. Heck *et al.* Wissenschaftliche Berichte, Forschungszentrum Karlsruhe FZKA 6019 (1998).
[22] M. Giller and G. Wieczorek, Astropart. Phys. 31 (2009) 212.
[23] P. Abreu *et al.* (Pierre Auger Collab.), JCAP 1111 (2011) 022.
[24] R. Ulrich, http://www-ik.fzk.de/∼rulrich/coast/, 2011.
[25] National Aeronautics and Space Administration (NASA), NASA-TM-X-74335, 1976.